Physica D 258 (2013) 61–76

Contents lists available at SciVerse ScienceDirect

Physica D

journal homepage: www.elsevier.com/locate/physd

Blended reduced subspace algorithms for uncertainty quantification of quadratic systems with a stable mean state

Themistoklis P. Sapsis *, Andrew J. Majda

Courant Institute of Mathematical Sciences, New York University, 251 Mercer str., New York, 10012 NY, United States

HIGHLIGHTS

- Generic limitations of order-reduction schemes for complex systems.
- Development of a blended method to overcome order-reduction limitations.
- Nonlinear statistical modeling of energy fluxes using reduced-order information.
- Illustration of the blended method in a triad model with strong cascade of energy.

ARTICLE INFO

Article history:
Received 6 September 2012
Received in revised form
14 March 2013
Accepted 3 May 2013
Available online 17 May 2013
Communicated by H.A. Dijkstra

Keywords:
Uncertainty quantification
Statistical modeling of nonlinear energy fluxes
Limitations of reduced-order models
Blended stochastic methods
Gaussian closure
Dynamical orthogonality

ABSTRACT

Order-reduction schemes have been used successfully for the analysis and simplification of high-dimensional systems exhibiting low-dimensional dynamics. In this work, we first focus on presenting generic limitations of order-reduction techniques in systems with stable mean state that exhibit irreducible high-dimensional features such as non-normal dynamics, wide energy spectra, or strong energy cascades between modes. The reduced-order framework that we consider to illustrate these limitations is the dynamically orthogonal (DO) field equations. This framework is applied to a series of examples with stable mean state, including a linear non-normal system, and a nonlinear triad system in various dynamical configurations. After illustrating the weaknesses and generic limitations of order reduction, we develop a novel, two-way coupled, blended approach based on the quasilinear Gaussian (QG) closure and the DO field equations. The new method (QG–DO) overcomes the limitations of its two ingredients and achieves exceptional performance in the examples described previously as well as in other configurations with strongly transient character without using any tuned or adjustable parameters.

1. Introduction

Order-reduction schemes or reduced-order models (ROMs) have been a popular technique for the simplification and analysis of high-dimensional complex systems across many scientific and engineering disciplines. Schemes based on this approach are essentially relying on the projection of the original system into a 'suitable' set of modes representing important and essential components of the dynamics. Various approaches and rules have been developed for the choice, computation, or improvement of these modes, including empirical criteria such as energy-based proper orthogonal decomposition (POD) (see, for example, [1,2]), linear-operator-theoretic model reduction methods, such as the balanced POD [3,4], and, more recently, dynamically orthogonal (DO) field equations that follow from the original system equation [5,6].

In many cases these ROMs give satisfactory performance allowing for dramatic decrease of the associated computational cost. In addition, a reduced-order representation of the original system often allows for the understanding of the underlying physical mechanisms—an understanding that could not be achieved using full system realizations either due to the vast computational cost or due to the complexity induced by the high-dimensional phase space. Therefore, it is clear why, for a big variety of systems, order reduction is the indicated and most efficient method of analysis.

Despite these appealing properties, ROMs can suffer from severe limitations either (i) due to the wrong choice of the modes where projection is performed or (ii) by inherent system properties that make it essential to project over a very high-dimensional subspace (of the original phase space) in order to obtain representative dynamics in the ROM. The first cause may be overcome by carefully choosing and optimizing the modes where reduction is performed (see, e.g., [7–9]). The second cause,

* Corresponding author. Tel.: +1 516 9741545; fax: +1 212 995 4121.
E-mail address: sapsis@mit.edu (T.P. Sapsis).

0167-2789/$ – see front matter © 2013 Elsevier B.V. All rights reserved.
http://dx.doi.org/10.1016/j.physd.2013.05.004

however, may present significant difficulties even when the mean state is stable, and, as we will see, it may not allow for any kind of efficient order reduction. The present work focuses on systems with such inherent order-reduction limitations; we also assume that the finite size of the attractor is caused by external excitation (to some or all of the modes) and not by inherent system instabilities, i.e. we consider the case of systems with stable mean state.

To illustrate these limitations, we consider the recently developed reduced-order uncertainty quantification (UQ) framework based on the dynamical orthogonality condition [5]—this is a closed set of equations that allows for the coupled evolution of the mean state, the shape of the modes, and the stochastic information in the reduced-order subspace. In addition, it contains both the POD method and the polynomial-chaos (PC) method as special cases. In order to quantify the performance of any ROM, we need a suitable stochastic framework that will 'measure' the different kinds of deviation that an ROM approximation may exhibit from the original system—this is formulated in Section 3, and it is a suitable modification of the empirical information framework developed in [10–12] for the quantification and improvement of model errors in climate science.

In Section 4 of this work, we investigate and document representative examples illustrating systems that do not allow for a typical Galerkin projection to a reduced-order subspace. Those examples are low-dimensional linear and nonlinear dynamical systems, motivated by physical situations associated with fluid flow phenomena such as tracer advection in a turbulent jet stream (modeled by a linear system with non-normal dynamics) [13, 10], as well as wide-range energy spectra and energy cascades between modes in turbulent flows (modeled by a triad system in various configurations). The last case that mimics energy cascades in turbulent flows is particularly instructive, since it illustrates in a clear way that omitting modes with respect to their energy content can lead to errors that are an order of magnitude larger than the omitted energy. For all these examples we derive the DO equations, and we use the formulated reduced-order empirical information framework to understand the limitations and reasons for failure of the reduction process.

In Section 5, we develop a blended approach based on the quasilinear Gaussian (QG) closure [11] and the DO method. This combined approach overcomes the limitations of each of its two ingredient methods. As we show, it allows for the inexpensive second-order modeling of a very large number of modes while at the same time it provides, in a fully coupled fashion, a high-order statistical modeling of a few important modes. The two-way coupling between the QG and the DO models occurs (i) through the nonlinear energy fluxes acting on the QG equations, computed through the third-order statistical structure inside the DO subspace, and (ii) through the QG mean state, over which the DO equations are computed. In Section 6, we illustrate the very good performance of the new blended approach in a variety of time-dependent and time-independent examples exhibiting the inherent limitations for order reduction described previously.

2. UQ based on dynamical orthogonality—a critical overview

2.1. System setup and exact statistical dynamics

We start by providing the general setup which will be a finite-dimensional system with linear dynamics and an energy-preserving quadratic part. More specifically, the general system that we consider is given by

$$\frac{d\mathbf{u}}{dt} = [L+D]\,\mathbf{u} + B(\mathbf{u},\mathbf{u}) + \mathbf{F}(t) + \dot{W}_p(t;\omega)\,\sigma_p(t) \tag{1}$$

acting on $\mathbf{u} \in \mathbb{R}^N$. In the above equation, the repeated index p indicates summation from 1 to P. This index will be used exclusively for this range of summation. Also, for every p, $W_p(t;\omega)$ is a standard Wiener process and $\sigma_p(t)$ is a scalar function. Although our analysis and results will be presented for system (1), the proposed methodology can be applied to more generic cases such as higher-order nonlinearities and multiplicative noise.

In the above equation, we have the following.

- L is a skew-symmetric linear operator representing the β-effect of Earth's curvature, topology, etc., and satisfying

  $L^* = -L$.

- D is a negative definite symmetric operator,

  $D^* = D$,

  representing dissipative processes such as surface drag, radiative damping, and viscosity.

The quadratic operator $B(\mathbf{u},\mathbf{u})$ conserves the energy by itself, so it satisfies

$$B(\mathbf{u},\mathbf{u})\cdot\mathbf{u} = 0.$$

Finally, $\mathbf{F}(t) + \dot{W}_p(t;\omega)\,\sigma_p(t)$ represents the effect of external forcing i.e. solar forcing, which we will assume can be split into a mean component $\mathbf{F}(t)$ and a stochastic component with white noise characteristics.

We use a finite-dimensional representation of the stochastic field consisting of fixed-in-time, N-dimensional, orthonormal basis

$$\mathbf{u}(t) = \bar{\mathbf{u}}(t) + \sum_{i=1}^{N} Z_i(t;\omega)\,\mathbf{v}_i,$$

where $\bar{\mathbf{u}}(t)$ represent the ensemble average of the response, i.e. the mean field, and $Z_i(t;\omega)$ are stochastic processes. Note that the indices i, j, k will be used as repeated indices to indicate summation from 1 to N.

The exact mean field equation is given by

$$\frac{d\bar{\mathbf{u}}}{dt} = [L+D]\,\bar{\mathbf{u}} + B(\bar{\mathbf{u}},\bar{\mathbf{u}}) + R_{ij}B(\mathbf{v}_i,\mathbf{v}_j) + \mathbf{F}, \tag{2}$$

where we have the covariance matrix given by $R_{ij} = \langle Z_i Z_j\rangle$, and $\langle\cdot\rangle$ denotes averaging over the ensemble members ω.

Moreover, the random component of the solution, $\mathbf{u}' = Z_i(t;\omega)\,\mathbf{v}_i$, satisfies

$$\begin{aligned}\frac{d\mathbf{u}'}{dt} &= [L+D]\,\mathbf{u}' + B(\bar{\mathbf{u}},\mathbf{u}') + B(\mathbf{u}',\bar{\mathbf{u}}) + B(\mathbf{u}',\mathbf{u}') \\ &\quad - R_{jk}B(\mathbf{v}_j,\mathbf{v}_k) + \dot{W}_p(t;\omega)\,\sigma_p(t).\end{aligned} \tag{3}$$

By projecting the above equation to each basis element $\mathbf{v}_i$, we obtain

$$\begin{aligned}\frac{dZ_i}{dt} &= Z_j\left([L+D]\,\mathbf{v}_j + B(\bar{\mathbf{u}},\mathbf{v}_j) + B(\mathbf{v}_j,\bar{\mathbf{u}})\right)\cdot\mathbf{v}_i \\ &\quad + \left(B(\mathbf{u}',\mathbf{u}') - R_{jk}B(\mathbf{v}_j,\mathbf{v}_k)\right)\cdot\mathbf{v}_i + \dot{W}_p\sigma_p\cdot\mathbf{v}_i.\end{aligned} \tag{4}$$

From the last equation, we directly obtain the exact evolution of the covariance matrix $R = \langle \mathbf{Z}\mathbf{Z}^*\rangle$:

$$\frac{dR}{dt} = L_v R + R L_v^* + Q_F + Q_\sigma, \tag{5}$$

where we have the following:

(i) the linear dynamics operator expressing energy transfers between the mean field and the stochastic modes (effect due to B), as well as energy dissipation (effect due to D) and non-normal dynamics (effect due to L, D, $\bar{\mathbf{u}}$)

$$\{L_v\}_{ij} = \left([L+D]\,\mathbf{v}_j + B(\bar{\mathbf{u}},\mathbf{v}_j) + B(\mathbf{v}_j,\bar{\mathbf{u}})\right)\cdot\mathbf{v}_i, \tag{6}$$

(ii) the positive definite operator expressing energy transfer due to external stochastic forcing

$$\{Q_\sigma\}_{ij} = \left(\mathbf{v}_i \cdot \sigma_p\right)\left(\sigma_p \cdot \mathbf{v}_j\right), \tag{7}$$

(iii) the energy flux between different modes due to non-Gaussian statistics (or nonlinear terms) given exactly through third-order moments

$$Q_F = \sum_{k_1,k_2=1}^{N} \left\langle Z_{k_1} Z_{k_2} Z_j \right\rangle B\left(\mathbf{v}_{k_1}, \mathbf{v}_{k_2}\right) \cdot \mathbf{v}_i + \sum_{k_1,k_2=1}^{N} \left\langle Z_{k_1} Z_{k_2} Z_i \right\rangle B\left(\mathbf{v}_{k_1}, \mathbf{v}_{k_2}\right) \cdot \mathbf{v}_j. \tag{8}$$

The last term involves higher-order statistics, and therefore suitable closure assumptions need to be made in order to set up a UQ scheme. The above exact statistical equations will be the starting point for the approximation schemes that we will develop and present below.

2.2. Overview of the DO order-reduction method for quadratic systems

Order-reduction techniques for UQ are based on the assumption that the modes that carry small amounts of energy do not have important influence on the global dynamics of the stochastic system. Although in some systems this may indeed be true, there are situations such as a typical turbulent dynamical system where many low-energy modes act as channels of energy, i.e. they either transfer or dissipate important amounts of energy, and therefore their effect has to be considered in the UQ scheme despite their small energy content.

From an energy transfer point of view, a reduced-order representation of the solution would ultimately lead to incomplete modeling of the nonlinear fluxes Q_F (Eq. (8)). Moreover, from the definition of the nonlinear fluxes it is clear that, even if a mode has low energy, its joint third-order moment with a high-energy mode may still be significant, a condition that describes the case where we have large energy flux from a high-energy mode to a low-energy mode. Finally, in addition to the incomplete modeling of the nonlinear energy transfer mechanism, a reduced-order representation may lead to incomplete description of the linear dynamics, since some unstable or oscillatory modes may be missing from the analysis.

Here, we illustrate these limitations using the recently developed UQ approach based on the dynamically orthogonal (DO) equations [5] that has been applied successfully to low Reynolds number flows having a very small number of instabilities [14–16]. The choice of the DO method as the illustrative order-reduction technique in this paper follows both from its adaptive character (time-dependent, dynamically evolving modes) and its generality (under appropriate conditions it reproduces both the POD method and the PC method). This stochastic framework is based on a reduced-order representation of the stochastic solutions with modes that have time dependence defined by an exact set of equations that follow from the full-system equation. The stochastic coefficients are obtained by Galerkin projection to these time-dependent modes, and together with the mean field equation they form a non-Gaussian reduced-order UQ scheme.

We proceed by formulating the DO system of equations for system (1). In particular, we use the DO representation

$$\mathbf{u}(t) = \bar{\mathbf{u}}(t) + \sum_{m=1}^{s} Y_m(t;\omega)\,\mathbf{e}_m(t), \tag{9}$$

where $\mathbf{e}_m(t)$, $m = 1, \ldots, s$ are time-dependent DO modes, defining the time-dependent subspace V_s, and $s \ll N$ is the reduction order. In what follows, the repeated indices l, m, n will be used to indicate summation from 1 to s.

The system operator will take the reduced-order form

$$\frac{d\mathbf{u}}{dt} = [L+D]\,\bar{\mathbf{u}} + B(\bar{\mathbf{u}},\bar{\mathbf{u}}) + \mathbf{F} + \dot{W}_p\sigma_p + [L+D]\,Y_m\mathbf{e}_m + Y_m\left(B(\bar{\mathbf{u}},\mathbf{e}_m) + B(\mathbf{e}_m,\bar{\mathbf{u}})\right) + Y_mY_nB(\mathbf{e}_m,\mathbf{e}_n).$$

From the above equation, we can already observe the incomplete modeling of both the linear and quadratic terms (described only along the directions $\mathbf{e}_m$). Using the DO equations, we obtain [5] the closed set of equations

- *Equation for the mean*

$$\frac{d\bar{\mathbf{u}}}{dt} = [L+D]\,\bar{\mathbf{u}} + B(\bar{\mathbf{u}},\bar{\mathbf{u}}) + C_{mn}B(\mathbf{e}_m,\mathbf{e}_n) + \mathbf{F}. \tag{10}$$

- *Equation for the stochastic coefficients*

$$\frac{dY_l}{dt} = Y_m\left([L+D]\,\mathbf{e}_m + B(\bar{\mathbf{u}},\mathbf{e}_m) + B(\mathbf{e}_m,\bar{\mathbf{u}})\right)\cdot\mathbf{e}_l + \left(Y_mY_n - C_{mn}\right)B(\mathbf{e}_m,\mathbf{e}_n)\cdot\mathbf{e}_l + \dot{W}_p\sigma_p\cdot\mathbf{e}_l. \tag{11}$$

The last equation can also be described in terms of the corresponding Fokker–Planck equation governing the probability density function $p_Y(\mathbf{y},t)$:

$$\frac{\partial p_Y}{\partial t} = -\mathrm{div}_y\left(\left(y_m\left([L+D]\,\mathbf{e}_m + B(\bar{\mathbf{u}},\mathbf{e}_m) + B(\mathbf{e}_m,\bar{\mathbf{u}})\right) + \left(y_my_n - C_{mn}\right)B(\mathbf{e}_m,\mathbf{e}_n)\right)\cdot\mathbf{e}_l p_Y\right) + \frac{1}{2}\mathrm{div}_y\nabla_y\left(Q_\sigma p_Y\right),$$

where, in (10) and (11), $C_{mn} = \langle Y_mY_n\rangle$ is the covariance matrix in the subspace.

- *Equation for the basis of the stochastic subspace*

Finally, for the equation describing the stochastic basis, we first compute the quantity $\langle\mathcal{L}[\mathbf{u}]\,Y_n\rangle\,C_{mn}^{-1}$, where $\mathcal{L}[\mathbf{u}]$ denotes the right-hand side of Eq. (1). A direct calculation gives

$$\langle\mathcal{L}[\mathbf{u}]\,Y_n\rangle\,C_{mn}^{-1} = [L+D]\,\mathbf{e}_m + B(\bar{\mathbf{u}},\mathbf{e}_m) + B(\mathbf{e}_m,\bar{\mathbf{u}}) + \sum_{n_1,n_2,n_3=1}^{s} B\left(\mathbf{e}_{n_2},\mathbf{e}_{n_3}\right)\left\langle Y_{n_1}Y_{n_2}Y_{n_3}\right\rangle C_{mn_1}^{-1}.$$

Therefore, the modes will evolve according to the equation

$$\frac{\partial\mathbf{e}_l}{\partial t} = [L+D]\,\mathbf{e}_l + B(\bar{\mathbf{u}},\mathbf{e}_l) + B(\mathbf{e}_l,\bar{\mathbf{u}}) + \sum_{n_1,n_2,n_3=1}^{s} B\left(\mathbf{e}_{n_2},\mathbf{e}_{n_3}\right)\left\langle Y_{n_1}Y_{n_2}Y_{n_3}\right\rangle C_{ln_1}^{-1} - \mathbf{e}_m\left(\left[L+D\right]\mathbf{e}_l + B(\bar{\mathbf{u}},\mathbf{e}_l) + B(\mathbf{e}_l,\bar{\mathbf{u}}) + \sum_{n_1,n_2,n_3=1}^{s} B\left(\mathbf{e}_{n_2},\mathbf{e}_{n_3}\right)\left\langle Y_{n_1}Y_{n_2}Y_{n_3}\right\rangle C_{ln_1}^{-1}\right)\cdot\mathbf{e}_m. \tag{12}$$

To understand better the limitations introduced by the reduction process, we formulate the equation for the covariance R. This follows from the reduced-order equation (11). Recalling that $\mathbf{e}_m = \sum_{k=1}^{N}(\mathbf{e}_m\cdot\mathbf{v}_k)\,\mathbf{v}_k$, we will have the reduced-order covariance equation

$$\frac{dR}{dt} = PL_{v,R}P^*R + RPL_v^*P^* + Q_\sigma + Q_{F,s},$$

where

(i) P is the projection matrix from $\mathbb{R}^N$ to $\mathbb{R}^s$,

$$P_{im} = \mathbf{v}_i\cdot\mathbf{e}_m, \quad i = 1,\ldots,N \text{ and } m = 1,\ldots,s,$$

(ii) $L_{v,s}$ is the reduced-order linear dynamics,

$$\left\{L_{v,s}\right\}_{mn} = \left([L+D]\,\mathbf{e}_n + B\left(\bar{\mathbf{u}}, \mathbf{e}_n\right) + B\left(\mathbf{e}_n, \bar{\mathbf{u}}\right)\right)\cdot \mathbf{e}_m, \quad m, n = 1, \ldots, s,$$

(iii) $Q_{F,s}$ is the matrix of the reduced-order nonlinear fluxes,

$$\left\{Q_{F,s}\right\}_{ij} = \left\langle Y_m Y_n Y_l \right\rangle \Big[\left(B\left(\mathbf{e}_m, \mathbf{e}_n\right)\cdot \mathbf{v}_i\right)\left(\mathbf{v}_j \cdot \mathbf{e}_l\right) + \left(B\left(\mathbf{e}_m, \mathbf{e}_n\right)\cdot \mathbf{v}_j\right)\left(\mathbf{v}_i \cdot \mathbf{e}_l\right)\Big], \quad i, j = 1, \ldots, N.$$

By examining the reduced-order form, we see that, even if the modes $\mathbf{e}_m$ span all the unstable directions of the linear operator, there might be non-normal dynamics which are not modeled, as well as dissipation of energy that is not taken into account (since many of the stable modes are not included in the linear dynamics). This is also the case with stable modes that return important amounts of energy to the mean field. On the other hand, the reduced-order nonlinear energy fluxes $Q_{F,s}$ only partially model the nonlinear energy transfers, since they only involve energy transfers between the subspace V_s and not energy interactions over the complete phase space.

Although for a system that possess a low-dimensional attractor the above scheme may have good UQ properties, for a system in which a large number of modes participates in strong energy transfers and dissipation we will need a vast number of modes in order to get satisfactory UQ properties. However, modeling a vast number of modes in a fully nonlinear fashion is not efficient, not feasible (for realistic systems), and, as we will see in Section 5, not necessary.

3. An empirical information framework for UQ using order-reduction methods

To quantify the performance of the order reduction, we will use the empirical information-theoretic framework [10–12]. Let υ denote the full solution of the original stochastic differential equation (SDE). Through the DO framework (or any other ROM), we obtain a reduced-order solution $\mathbf{u}$ (see representation (9)) that 'lives' in the reduced-order stochastic subspace V_s of dimensionality s. The projection of any field quantity υ into the stochastic subspace V_s is given by $P^*\upsilon$, where P is the mode matrix defined in the previous section.

There are several sources of error between the full solution υ and its reduced-order approximation $\mathbf{u}$. Since the full solution lives in an N-dimensional space while the reduced-order solution is restricted to the much smaller s-dimensional space, a natural question to ask is what we 'lose' by performing this reduction. In other words, what is the amount of inaccessible information that lies in the orthogonal complement of the reduced-order subspace?

The next question to ask is how well we are doing in the reduced-order subspace. In particular, how close is the projection of the reduced-order solution $\mathbf{u}$ to the full solution $P^*\upsilon$? This is a question that can be answered in a straightforward manner by using the empirical information framework. Note that the above two sources of error do not include the distance of the mean fields in the orthogonal complement since, as we will see, this is not expressed through the amount of inaccessible information, and of course it cannot be quantified by the distance of the two solutions in the reduced-order subspace.

(A) *Error within the subspace.*

This error involves the distance between the exact full solution and the reduced-order approximation, as this is measured in the reduced-order stochastic subspace. We compute directly the relative entropy between the projection of the full solution $P^*\upsilon$ and the reduced-order solution projected to the stochastic subspace $P^*\mathbf{u}$ (note that the projection in the second case involves only the mean value which lives into the full space). In this way, we obtain

$$\mathcal{P}\left(P^*\upsilon, P^*\mathbf{u}\right) = \int_{\mathbb{R}^s} p_{\upsilon,\mathbf{v}_s} \log \frac{p_{\upsilon,\mathbf{v}_s}}{p_{\mathbf{u}}}, \tag{13}$$

where $p_{\upsilon,\mathbf{v}_s}$ is the probability density function (pdf) for the projection $P^*\upsilon$ and $p_{\mathbf{u}}$ is the pdf for $P^*\mathbf{u}$. The last quantity is always positive, and it expresses the quality of the approximation within the stochastic subspace.

Assuming Gaussian statistics, the above expression takes the more explicit form

$$\mathcal{P}\left(P^*\upsilon, P^*\mathbf{u}\right) = \left[\frac{1}{2}\left(\bar{\upsilon}^* - \bar{\mathbf{u}}^*\right) P\mathbf{C}_{YY}^{-1}P^*\left(\bar{\upsilon} - \bar{\mathbf{u}}\right)\right] + \left[-\frac{1}{2}\log\det\left(P^*\mathbf{C}_{\upsilon\upsilon}P\mathbf{C}_{YY}^{-1}\right) + \frac{1}{2}\left(\mathrm{tr}\left(P^*\mathbf{C}_{\upsilon\upsilon}P\mathbf{C}_{YY}^{-1}\right) - s\right)\right]. \tag{14}$$

The first term in (14) is the signal which measures normalized errors in the mean, while the second term is the dispersion which measures information-theoretic errors in the variance [13,10,12].

(B) *L^2 distance between the mean fields in $\mathbf{V}_s^\perp$.*

The next step involves the quantification of error in the orthogonal complement of $\mathbf{V}_s$. The reduced-order model provides, in the orthogonal complement, information only for the mean field. Therefore, the first step to quantify the performance of the reduction is to measure the distance between the mean field produced by the approximation and the exact one, both projected to the orthogonal complement. To achieve this, we consider the ad hoc metric that expresses the distance of the two solutions in $\mathbf{V}_s^\perp$:

$$d_{\mathbf{V}_s^\perp}\left(\mathbf{u}, \upsilon\right) = \frac{1}{2}\left\|\left(I - P^*\right)\left(\bar{\upsilon} - \bar{\mathbf{u}}\right)\right\|^2.$$

(C) *Lack of information due to the reduction.* We measure the uncertainty that we 'lose' due to the reduction using second-order statistical properties of the pdfs involved, and more specifically by using the Frobenius norm of the square root of $\mathbf{C}_{\upsilon\upsilon}$. In particular, we define $Q_C \in \mathbb{R}^{N\times N}$ as

$$Q_C^2 = \mathbf{C}_{\upsilon\upsilon}.$$

Then, the quantity δS_V^F, which will measure the uncertainty outside $\mathbf{V}_S$, is defined through the Frobenius norm $\|\cdot\|_F$:

$$\delta S_V^F \equiv \{\textit{total variance}\} - \{\textit{total variance in } \mathbf{V}_S\} = \|Q_C\|_F^2 - \left\|P^*Q_C\right\|_F^2 = \sum_{i=1}^{N}\sigma_i^2 - \sum_{m=1}^{s}\tilde{\sigma}_m^2 \geq 0, \tag{15}$$

where σ_i^2 and $\tilde{\sigma}_i^2$ are the eigenvalues of $\mathbf{C}_{\upsilon\upsilon}$ and $P^*\mathbf{C}_{\upsilon\upsilon}P$, respectively. To prove the positivity of this quantity, we first denote as $P^\perp \in \mathbb{R}^{N\times N-s}$ the matrix that contains the basis elements that span $\mathbf{V}_s^\perp$. We also use the orthogonal matrix $\tilde{P} = \left[P|P^\perp\right]$, for which we have

$$\|Q_C\|_F^2 = \mathrm{trace}\left(Q_C Q_C^*\right) = \mathrm{trace}\left(Q_C\tilde{P}\tilde{P}^*Q_C^*\right) = \left\|\tilde{P}^*Q_C\right\|_F^2.$$

Furthermore, we have

$$\left\|\tilde{P}^*Q_C\right\|_F^2 = \sum_{i=1}^{N}\sum_{j=1}^{N}\left(\sum_{k=1}^{N}\tilde{P}_{ik}Q_{C,kj}\right)^2 \geq = \sum_{m=1}^{s}\sum_{j=1}^{N}\left(\sum_{k=1}^{N}P_{mk}Q_{C,kj}\right)^2 = \left\|P^*Q_C\right\|_F^2.$$

This proves the positivity of δS_V^F. Note that equality is achieved if and only if the directions that correspond to the orthogonal complement are associated with zero variance.

4. Inherent limitations of order-reduction methods for systems with stable mean state

We will now focus on systems with irreducible features such as non-normal dynamics or strong nonlinear energy transfer properties. These features are typical in many physical applications, and, as we will see, they often cause failure of the order-reduction procedure.

The first example will be an exactly solvable, linear, non-normal system. Non-normal systems are characterized by the non-commutability of L and L^*. A typical example of such a system is advection of a passive tracer in a turbulent jet, where even though the tracer advection depends strongly on the flow field the opposite is not true. This one-way dependence of the dynamical variables is expressed as a strong asymmetry in the linear dynamics [13,10].

The second example will be a low-dimensional quadratic system with energy-conserving quadratic terms. In particular, we will consider the triad system [17–20] in various configurations that mimic strongly nonlinear dynamical mechanisms such as irreversible energy transfer between modes. The last example will be of particular importance, since it will illustrate very clearly that the energy content of a mode may be an incorrect indicator for its importance in the global system dynamics.

4.1. Limitation in skill due to non-normal linear dynamics

To illustrate the irreducible character of a non-normal dynamical feature, we consider a linear two-dimensional (2D) SDE problem [13]. The goal is to reveal and understand the limitations of the reduction method,and we will start from this simple system since most of the derivations can be done analytically.

$$dx = (-ax + \epsilon_1 y)\, dt$$
$$dy = (\epsilon_2 x - by)\, dt + \sigma dW(t).$$

We will perform reduction in a 1D subspace. In this case, the equation for the mode $\mathbf{e}_1(t) = (x_1(t), y_1(t))^T$ will take the form

$$\frac{d\mathbf{e}_1}{dt} = A\mathbf{e}_1 - \left(\mathbf{e}_1^T A \mathbf{e}_1\right)\mathbf{e}_1,$$

where $A = \begin{pmatrix} -a & \epsilon_1 \\ \epsilon_2 & -b \end{pmatrix}$. Since the above equation preserves the magnitude, $\|\mathbf{e}_1\| = 1$, we may represent the DO vector in polar coordinates as $\mathbf{e}_1(t) = (\sin\theta(t), \cos\theta(t))^T$. In this way, we can solve the mode equation exactly, to obtain

$$\int_{\theta_0}^{\theta(t)} \frac{d\theta}{(b-a)\sin\theta\cos\theta + \epsilon_1\cos^2\theta - \epsilon_2\sin^2\theta} = t - t_0.$$

The steady-state values θ_∞ may also be obtained:

$$\tan\theta_\infty = \frac{(b-a) \pm \sqrt{(a-b)^2 + 4\epsilon_1\epsilon_2}}{2\epsilon_2}.$$

One of these solutions is dynamically stable and the other is not. Therefore, the mode is characterized by a unique equilibrium that depends only on the system parameters and not the excitation intensity. The next step is to understand how the variance evolves in this reduced-order 1D subspace. The equation for the variance $C_{YY}(t)$ has the simple form (obtained through Eq. (11) after algebraic manipulations)

$$\frac{dC_{YY}(t)}{dt} = -2\left(a\sin^2\theta + b\cos^2\theta - (\epsilon_1+\epsilon_2)\sin\theta\cos\theta\right) \times C_{YY}(t) + \sigma^2\cos^2\theta.$$

From the last equation we may also obtain the steady-state value of the variance (inside the stochastic subspace):

$$C_{YY\infty} = \frac{\sigma^2}{2\left(a\tan^2\theta_\infty + b - (\epsilon_1+\epsilon_2)\tan\theta_\infty\right)}.$$

The extreme non-normal case will be characterized by $\epsilon_1 \neq 0$, and $\epsilon_2 = 0$. Here, we will focus on a 'smoother' case where $\epsilon_2 = \epsilon_1^{-1} = \epsilon^{-1}$, where ϵ could have both large and small values. This way, we will be able to observe the transition in the UQ performance as we move to more non-normal regimes.

To measure the performance of the reduction process, we will compare with the exact solution. For the linear system under consideration, the exact stationary covariance matrix is given by [13]

$$C_{\upsilon\upsilon\infty} = \frac{\sigma^2}{2(a+b)(ab-1)}\begin{pmatrix} \epsilon^2 & \epsilon a \\ \epsilon a & a^2 + ab - 1 \end{pmatrix}.$$

By combining the above expressions for the exact covariance and the DO solution with the empirical information framework formulated in the previous section (Eqs. (13)–(15)), we obtain all the necessary measures to assess the performance of the reduction process. In Fig. 1, we present the performance of the reduction algorithm for different system parameters. We also show the amount of variance of the exact covariance matrix projected to the stochastic subspace and to its orthogonal complement. We observe that for large ϵ the reduction algorithm converges to the wrong subspace, since most of the uncertainty of the exact response is contained in the orthogonal complement. On the other hand, for small ϵ there are some locations in the parametric space where, even though the algorithm captures the correct subspace, the amount of covariance captured is not accurate (Fig. 1(a)).

In Fig. 2, we present the time evolution of the performance measures as well as of the exact covariance (projected to the stochastic subspace and its orthogonal complement). In the first case (left plot), the reduction algorithm predicts the right stochastic subspace and captures the variance very accurately. In the second case, however, the reduced-order subspace converges to the wrong direction, which is associated with the wrong amount of covariance, and thus the reduction scheme is inaccurate. In both cases, we pick an initial covariance matrix for the full system that has all of its variance concentrated in one direction, which coincides with the initial direction of the stochastic subspace.

4.2. Limitation in skill due to omitted energy or energy transfers

We continue our analysis by considering a simple but nevertheless instructive model, namely the triad system. This is a three-dimensional system with a quadratic part that is both divergence free and energy preserving. The linear part consists of a dissipative operator that is negative definite and a skew-symmetric operator. The nonlinear coupling in triad systems is generic of nonlinear coupling between any three modes in larger systems with quadratic nonlinearities [18–20]. We can think of this 'toy' problem as a poor man's approach to a full fluid system in which the nonlinear terms, dissipation, and skew-symmetric part represent respectively the advection terms, the viscous dissipation, and the Coriolis effect, while the stochastic noise represents the nonlinear interactions with other modes in a crude fashion. The goal here is to understand how the reduction performs over qualitatively different dynamical regimes of this system.

In particular, the system we consider is a three-dimensional special case of the generic quadratic system (1) given by

$$du_1 = (-\gamma_1 u_1 + \lambda_{12}u_2 + \lambda_{13}u_3 + \beta_1 u_3 u_2)\, dt + \sigma_1 dW_1 \quad (16a)$$
$$du_2 = (-\gamma_2 u_2 - \lambda_{12}u_1 + \lambda_{23}u_3 + \beta_2 u_1 u_3)\, dt + \sigma_2 dW_2 \quad (16b)$$
$$du_3 = (-\gamma_3 u_3 - \lambda_{13}u_1 - \lambda_{23}u_2 + \beta_3 u_2 u_1)\, dt + \sigma_3 dW_3, \quad (16c)$$

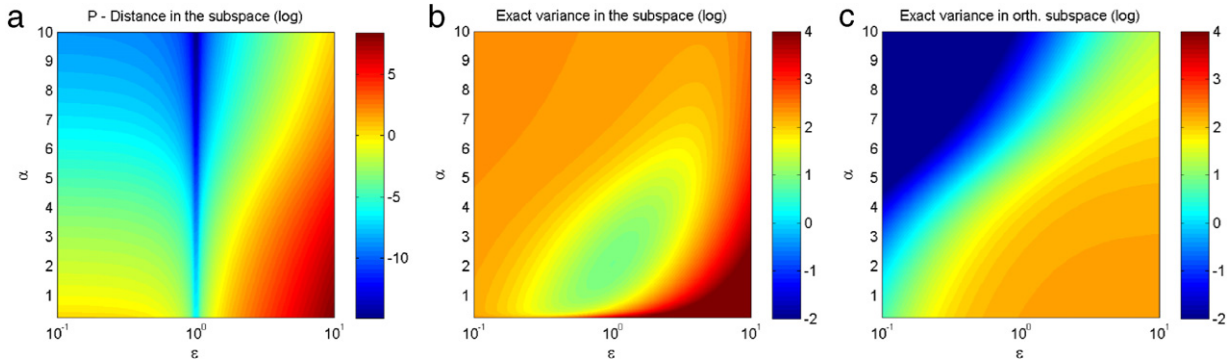

Fig. 1. Performance of reduction for $b = 5$ over different values of ϵ and a in the steady-state regime. (a) Information-theoretic distance $\lim_{t\to\infty} \log\left(\mathcal{P}\left(t\right)\right)$ within the stochastic subspace; (b) projection of true covariance in the stochastic subspace $\lim_{t\to\infty} \log(\mathbf{e}_1^T\left(t\right) C_{vv}\left(t\right) \mathbf{e}_1\left(t\right))$; (c) projection of the exact covariance in the orthogonal complement $\mathbf{V}_s^{\perp}$: $\lim_{t\to\infty} \log(\mathbf{e}_2^T\left(t\right) C_{vv}\left(t\right) \mathbf{e}_2\left(t\right))$.

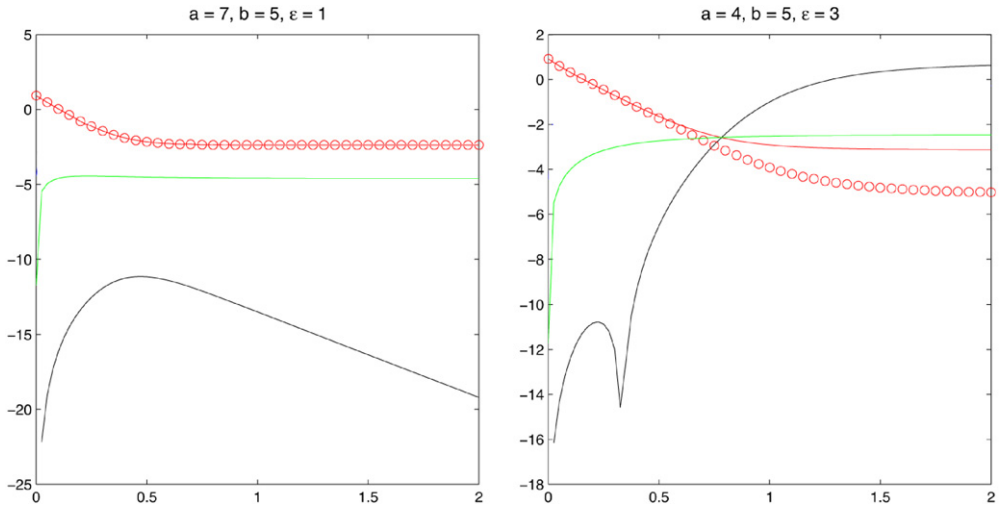

Fig. 2. Solid black line: information-theoretic distance $\log\left(\mathcal{P}\left(t\right)\right)$ within the stochastic subspace; solid red line: projection of true covariance in the stochastic subspace $\log(\mathbf{e}_1^T\left(t\right) C_{vv}\left(t\right) \mathbf{e}_1\left(t\right))$; red circles: covariance $\log(C_{YY}\left(t\right))$ in the subspace computed by the reduction method; green line: projection of the exact covariance in the orthogonal complement $\mathbf{V}_s^{\perp}$: $\log(\mathbf{e}_2^T\left(t\right) C_{vv}\left(t\right) \mathbf{e}_2\left(t\right))$, where $\mathbf{e}_2 \perp \mathbf{e}_1$. (For interpretation of the references to colour in this figure legend, the reader is referred to the web version of this article.)

with $\beta_1 + \beta_2 + \beta_3 = 0$. The case where $\frac{\sigma_1^2}{2\gamma_1} = \frac{\sigma_2^2}{2\gamma_2} = \frac{\sigma_3^2}{2\gamma_3} \equiv E$ is a special one, since in this symmetric situation the statistical system dynamics always converge at long times to an invariant measure that is Gaussian and with energy that is distributed equally among the three degrees of freedom. This invariant measure in this case is Gaussian, and is given by

$$p_Y = C \exp\left(-\frac{1}{2}\frac{\|\mathbf{u}\|^2}{E}\right).$$

From the form of the invariant measure, and in particular from its property with equipartition of energy in phase space, we anticipate that, even in the best case, the reduction algorithm will be able to capture only a fraction of the steady-state covariance ($\frac{1}{3}$ or $\frac{2}{3}$ depending on the number of modes used for the reduction) as times evolves.

4.2.1. Reduced-order modeling of the triad system using DO

We shall now compare the performance of the DO order reduction with the full Monte Carlo solution of the triad system for different parametric regimes. In particular, we choose parameters that correspond to three different dynamical regimes: the strong dissipation regime, the strongly nonlinear regime with equipartition of energy, and a strongly nonlinear regime with an energy cascade. These three cases are representative of a fluid system over different dynamical regimes characterized respectively by either laminar (but possibly unstable) features or strongly nonlinear (turbulent) dynamics with or without an energy cascade. For the numerical solution of the DO equations, we follow the approach presented in [5].

For a single-mode reduction, it can be easily seen that the statistics inside the subspace will evolve under the effect of linear dynamics alone, because in this case the DO equation (11) for the stochastic coefficient will take the linear form

$$\frac{dY_1}{dt} = Y_1\left(\left[L + D\right]\mathbf{e}_1 + B\left(\bar{\mathbf{u}}, \mathbf{e}_1\right) + B\left(\mathbf{e}_1, \bar{\mathbf{u}}\right)\right) \cdot \mathbf{e}_1 + \dot{W}_k \sigma_k \cdot \mathbf{e}_1, \tag{17}$$

since $B\left(\mathbf{e}_1, \mathbf{e}_1\right) \cdot \mathbf{e}_1 = 0$, and therefore all the quadratic terms in the equation vanish and the dynamics is linear. Therefore, this is an extreme form of order reduction in which we have complete suppression of the nonlinear energy transfer properties, since for Gaussian statistics the reduced-order fluxes $Q_{F,S}$ will vanish. In this section, we will present results for the DO approximation scheme with a single-dimensional stochastic subspace. Note however that two-mode DO reduction does not improve the performance, and the corresponding results for the same triad test problem are shown in Section 6 (Figs. 5, 6—top rows).

Case I: *strong dissipation regime*. The first case that we study is the one in which all terms have the same order of magnitude. We focus on two different temporal regimes: the transient state and the

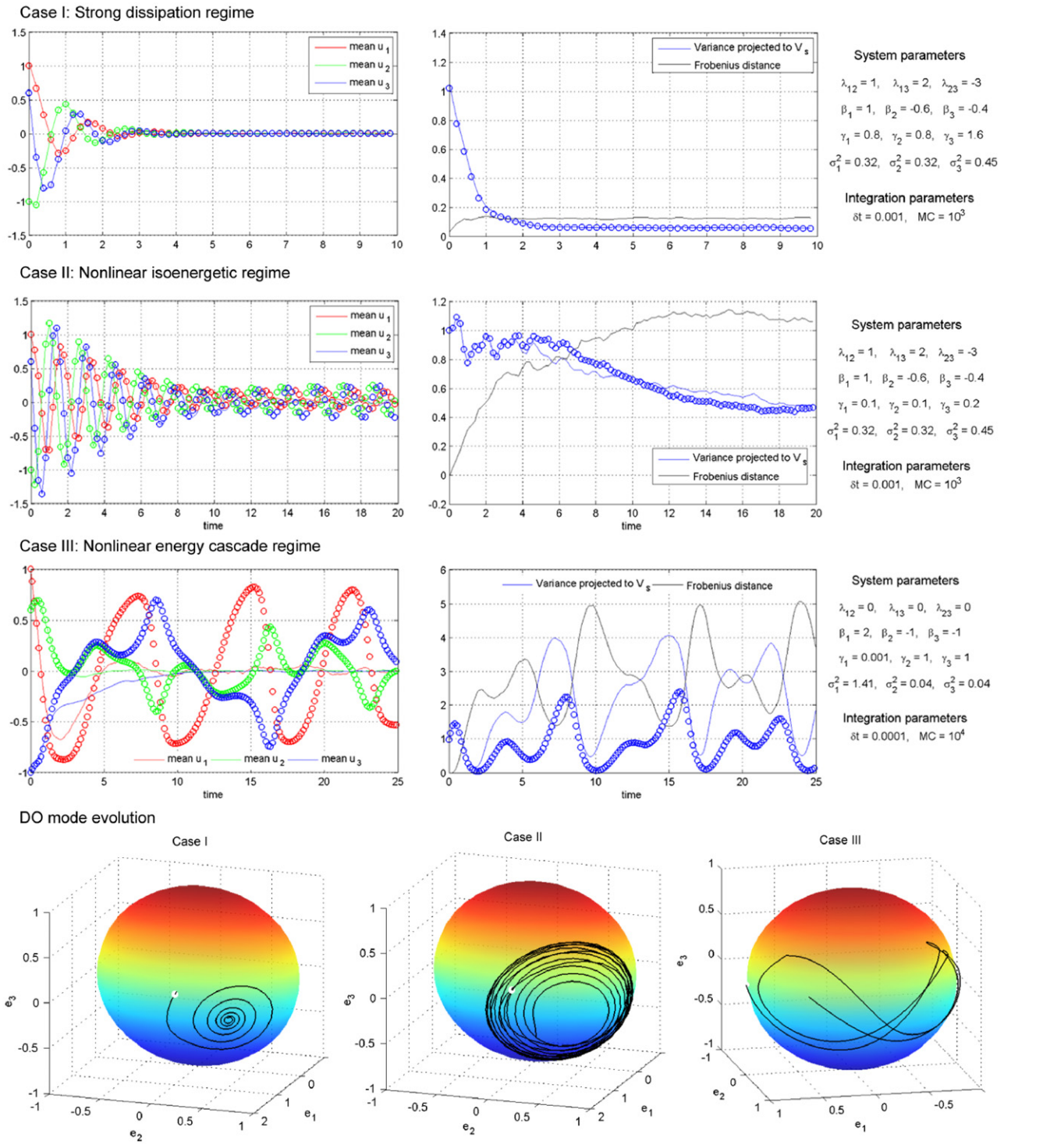

Fig. 3. Performance of the DO reduction for the triad system in three different dynamical regimes: strong dissipation regime (top row), nonlinear isoenergetic regime (second row), and nonlinear energy cascade regime (third row). The time evolution of the DO mode for each case is shown in the bottom plots.

steady state. In Fig. 3 (top-row), we present the system response—the solid lines in the left time-series plot represent the mean values of the three components of the solution $u_1,\ u_2,\ u_3$ computed with a direct Monte Carlo approach. The estimated mean values using the reduction technique are plotted as circles.

In the right plot, we show the comparison of the exact and reduced-order solutions in terms of the second-order characteristics. In particular, we present the projection of the full (Monte Carlo) covariance on the reduced-order subspace (solid blue line) superimposed with the variance $\langle Y_1^2 \rangle$, as this is computed through the reduced-order methodology. We also present the Frobenius distance δS_V^F defined in (15). Finally, in the bottom row we present the trajectory describing the evolution of the DO mode which 'lives' on the unit sphere—the white dot indicates the initial condition.

In this parametric regime, the reduction algorithm, even though it uses only one mode, does sufficiently well in approximating the state of the system both over the transient regime, where variance is important, and in the steady state. The magnitude of uncertainty in the reduced-order stochastic subspace is captured sufficiently well, even though the Frobenius distance indicates that

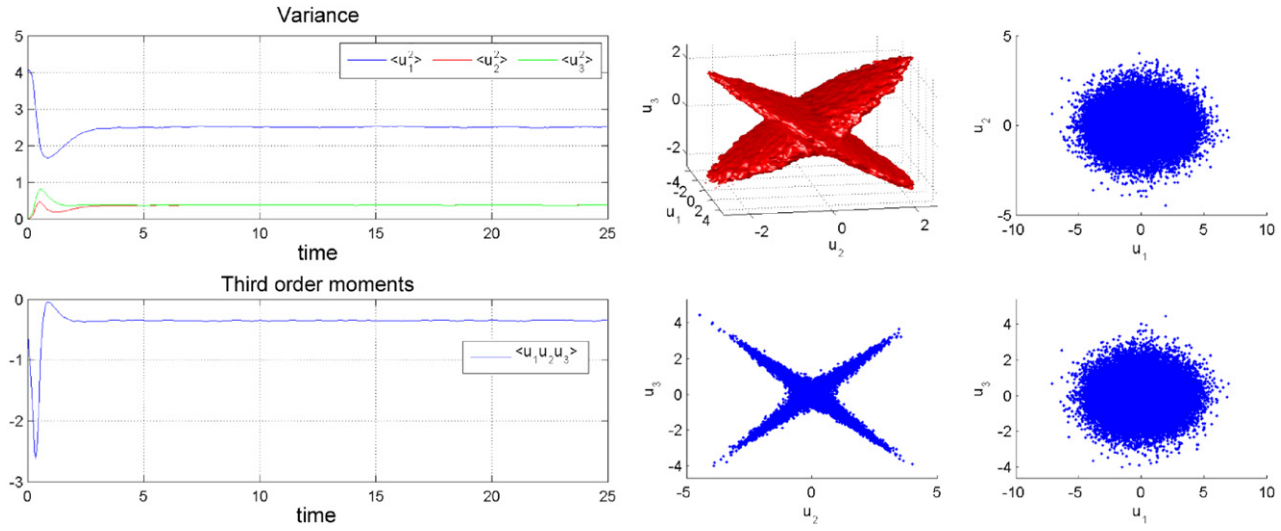

Fig. 4. Strongly nonlinear regime with an energy cascade: full-system statistics predicted with the direct Monte Carlo method in the original system. In the right plots, the steady-state conditional probability density functions of $p_{u_1u_2u_3}$ are shown as well as 2D scatter plots.

during the steady-state regime the resolved uncertainty is only $\frac{1}{3}$ of the full uncertainty, because the total variance in the statistical steady state is small in this weakly nonlinear regime. Here, $\frac{1}{3}$ is the maximum amount of variance that the reduction algorithm can capture, since one mode is used and the system parameters are such that equipartition of energy is reached in the steady state.

Case II: *strongly nonlinear regime with Gaussian steady state*

This case mimics dynamics with high Reynolds number which are still characterized by close-to-Gaussian statistics (see [12]). To model this regime, we set the damping in the system to be an order of magnitude smaller than all the other terms, making the steady-state variance an order of magnitude larger compared with the previous case. The results are shown in the second row of Fig. 3.

Even though the reduction captures the system dynamics satisfactorily during the initial phase, it begins to diverge when the system approaches the statistical steady-state regime. A more careful observation of the time series reveals that the divergence begins when the ignored covariance (expressed through the Frobenius distance) becomes important. When this happens, we first have a relatively small divergence of the subspace variance, and subsequently (when we have entered the steady-state regime) the estimated mean value performs high-amplitude oscillations around the true mean state. We also notice that, contrary to the previous case in which the single-mode approximation converged to a steady-state point, in this case the mode performs oscillations and it never reaches an equilibrium point. The observed deviation of the mean value is a direct consequence of the ignored covariance (due to the reduction), since in the full mean equation (2) this omitted covariance plays an important role, and its effect is proportional to the magnitude of the quadratic terms.

Case III: *strongly nonlinear regime with an energy cascade*.

This is the most representative regime for turbulent flows. We have strongly nonlinear dynamics, combined with strong energy transfers—a property that leads to strongly non-Gaussian statistics with a probability measure on the attractor that has a full measure but effective lower-dimensional support (Fig. 4). In particular, we consider a set of parameters similar to those used in [21] (shown in the third row of Fig. 3). Here, the background linear skew-symmetric operator vanishes and the first component is weakly damped and strongly forced by noise, while the second and third components are strongly damped, and the nonlinear interaction component of the first mode has opposite sign from the other two modes, so there is large energy in the first mode which is rapidly transferred to the other modes [19,20].

In Fig. 4, we present the statistics of the system as computed by the direct Monte Carlo method. Thus, in the statistical steady-state regime we have one mode carrying most of the system energy and two low-energy modes absorbing energy from the first one. This energy transfer property is manifested by the third-order moment $\langle u_1u_2u_3\rangle$ (shown in Fig. 4), whose negative value indicates the energy transfer from the first mode to the other two. This flow of energy is also illustrated by the nearly two-dimensional character of the joint probability density function (see [6] for a rigorous connection of the energy transfer properties and the dimensionality of the probability measure). This strongly nonlinear regime with an energy cascade has a Fokker–Planck equation with an elliptic generator with a smooth three-dimensional steady-state probability density which is nearly two dimensional.

Note that, since this is a system in which only one mode has important variance while the other two are much weaker in terms of energy, one may expect that it is an ideal candidate for single-mode order reduction. However, this is not the case. In Fig. 3, we present the results of the single-mode reduction and we compare with direct Monte Carlo simulation. We observe that we have very large discrepancies in both the first-order and second-order statistics. These discrepancies are much larger in magnitude than the order of the ignored variance.

The answer comes from the essentially irreducible character of the steady-state probability measure, which does not allow for any approximation by a single-mode system (or even two-mode reduction—see the results in Section 6). This is because the two low-energy modes play an important role in the global dynamics by extracting energy from the high-energy mode and strongly dissipating it. In particular, this non-Gaussian cross-correlation structure is responsible for the persistent energy transfer from mode 1 to modes 2 and 3, which, contrary to the magnitude of the modes 2 and 3, is very important. Ignoring one or both of these modes completely destabilizes the energy fluxes, and causes large errors in the eigenvalues of the covariance and subsequently the estimated mean.

The above instructive example illustrates very clearly that *the small magnitude of the uncertainty in specific directions may not always be an efficient criterion to neglect dynamics*. This is especially the case for turbulent flows where we have very strong energy transfers among scales (modes) that have to be modeled, even if the modes are associated with weak energy content.

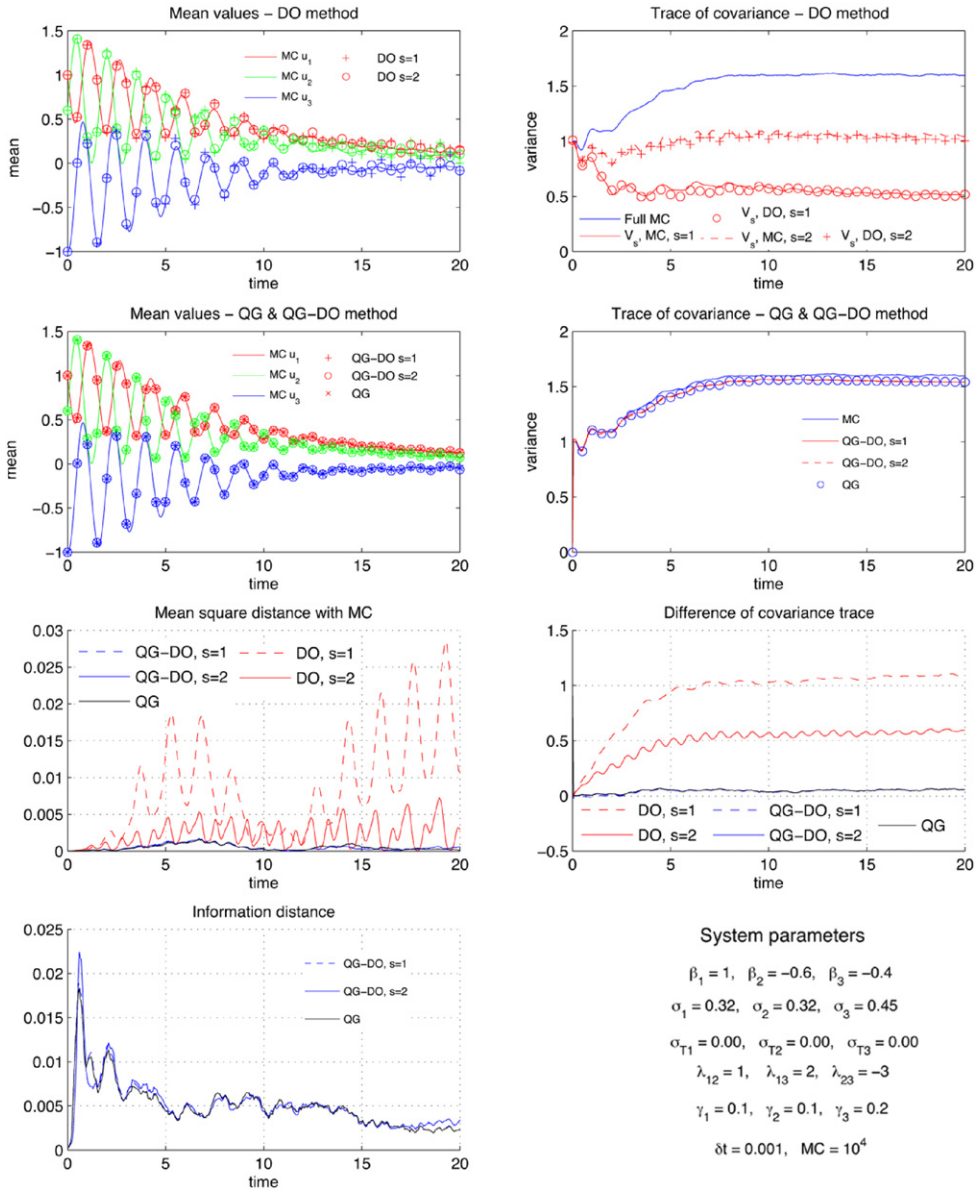

Fig. 5. Comparison of the considered UQ algorithms for the triad system in the strongly nonlinear regime with Gaussian steady state. The results are presented in terms of the first and second moments, and they are compared with direct Monte Carlo simulations.

5. A blended approach based on the quasilinear Gaussian method with DO energy fluxes: the QG–DO method

From the previous section, it is clear that in many applications of practical interest order-reduction approaches will fail to capture essentially irreducible dynamics such as non-normality features or energy cascade properties. This is due to the incorrect energy balance or fluxes caused by the ignored modes and the associated energy transfers. This limitation naturally leads us to consider simplified statistical dynamics in the larger phase space in our analysis. A relevant approach towards this direction is the quasilinear Gaussian (QG) closure, which we will briefly describe.

5.1. Overview of quasi-linear Gaussian (QG) closure schemes

The simplest closure scheme [11] for the moment problem stated in Section 2 is to completely neglect the third-order moments in the evolution equation for the covariance, i.e. set $Q_F = 0$. As illustrated in [13] and the references therein, this type of simple closure with augmented noise can handle UQ in systems with transient intermittent instabilities. This QG closure is equivalent with neglecting quadratic terms only in the equation for the covariance (partial linearization of the moment system) or by assuming Gaussian statistics. In this case, the evolution of the covariance matrix is performed with the closed set of equations

$$\frac{d\bar{\mathbf{u}}}{dt} = [L + D]\,\bar{\mathbf{u}} + B\,(\bar{\mathbf{u}}, \bar{\mathbf{u}}) + R_{ij}B\left(\mathbf{v}_i, \mathbf{v}_j\right) + \mathbf{F} \tag{18a}$$

$$\frac{dR}{dt} = L_v R + RL_v^* + Q_\sigma. \tag{18b}$$

Despite its simplicity, QG closure is characterized by some very important limitations, which are connected with the misleading modeling of the nonlinear energy fluxes (see [22] for a detailed illustration of these limitations). In particular, by completely ignoring the third-order moments, we neglect energy transfers due to nonlinear terms. In systems with inherent instabilities, these fluxes are responsible for the finite amount of energy in the unstable

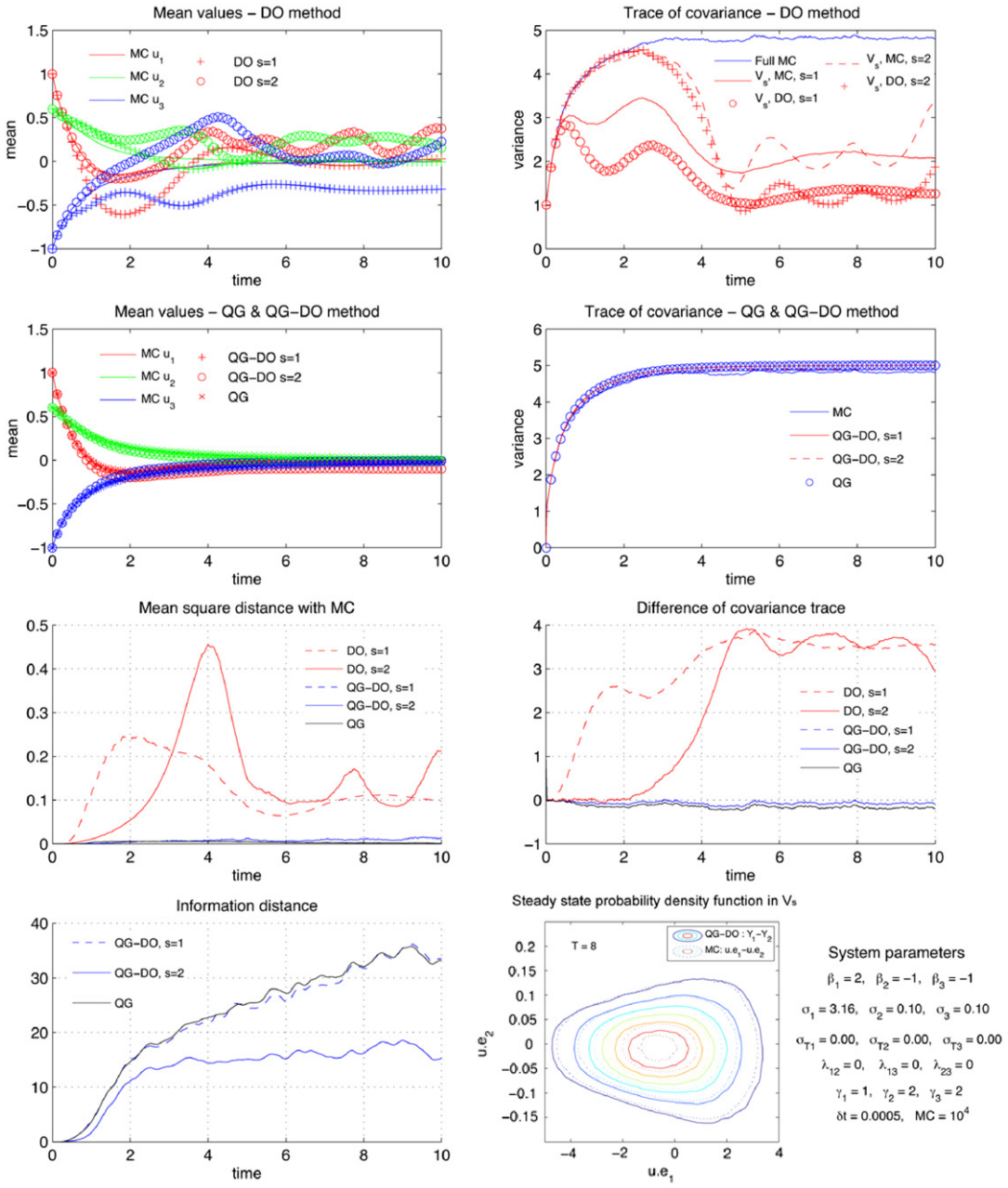

Fig. 6. Comparison of the considered UQ algorithms for the triad system in the strongly nonlinear regime with an energy cascade. The time-series results are presented in terms of the first and second moments, and they are compared with direct Monte Carlo simulations. The pdf in the steady-state DO subspace is shown and compared with the pdf computed through Monte Carlo simulations.

modes and non-zero energy in the stable modes [22]. In the context of systems with linearly stable mean state, nonlinear energy fluxes still play an important role, since this is the only means of energy transport from one mode to another (e.g. Case III in the previous section). Alternatively, a complete modeling of the nonlinear energy fluxes would require a vast amount of statistical information, which for systems with large phase space would be computationally intractable.

Therefore, on one hand we have the QG closure, which can handle a large part of the spectrum but ignores the non-Gaussian character of the statistics and the nonlinear nature of the dynamics which for some modes may play a crucial role. In other words, QG respects the dimensionality of the problem but fails to capture nonlinear energy exchanges between different modes. On the other hand, we have the reduced-order DO framework, which can fully handle the nonlinear non-Gaussian character of the dynamics, but only within a small part of the spectrum. This is because DO omits low-energy modes that can be important when they act as energy channels (e.g. non-normal systems, energy cascades, etc.).

The goal of the following section is to combine these two complementary approaches towards a new blended UQ strategy that will be able to handle both the irreducible features (such as non-normal dynamics) and the strongly nonlinear features such as non-Gaussian statistics. In particular, the basis of this blended method will be the evolution of the full system covariance (from now on called QG covariance) through Eq. (5), where the energy fluxes due to the nonlinear terms will be computed only in the reduced-order subspace. This idea combines the advantages of both methods, while it overcomes their disadvantages.

5.2. Description of QG–DO blended method

We will now present in detail the blended approach which combines the two models. The basic setup is to consider a small number of modes resolved with the DO equations (describing high-energy dynamics) coupled with a much larger number of modes which will not evolve in time and for which we will resolve only the second-order statistics. Essentially, we will have two coupled models propagating uncertainty. The fixed basis model (QG) will be used to evolve (i) the mean and (ii) the second-order statistics (using high-dimensional equations), and the time-dependent basis model will be used to compute (i) the non-Gaussian information for the high-energy modes, and (ii) the shape of the high-energy modes, as well as the third-order moments used for the computation of the energy flux between different modes.

The coupling between the two models will be naturally performed at two levels: (i) the evolution of the reduced-order dynamics (DO subspace and coefficients) using the mean field information obtained by the full mean field equation, and (ii) the evolution of the full (or QG) second-order statistics using energy fluxes computed by the reduced-order non-Gaussian (DO) statistical information.

We will use a double representation for the solution. Specifically, we will represent the solution to perform UQ through the QG representation that employes a fixed basis,

$$\mathbf{u}(t) = \bar{\mathbf{u}}(t) + \sum_{i=1}^{N} Z_i(t;\omega)\,\mathbf{v}_i,$$

while the representation of the uncertainty used to compute the energy fluxes due to nonlinearities and non-Gaussian statistics in the high-energy modes will be given by

$$\mathbf{u}(t) = \bar{\mathbf{u}}(t) + \sum_{m=1}^{s} Y_m(t;\omega)\,\mathbf{e}_m(t),$$

which is the reduced-order DO representation.

- *Mean field equation*

The mean field equation that we will employ is the one that takes into account the full covariance information—expressed through the QG covariance R. This is essentially the mean field equation for the fixed basis,

$$\frac{d\bar{\mathbf{u}}}{dt} = [L+D]\,\bar{\mathbf{u}} + B(\bar{\mathbf{u}},\bar{\mathbf{u}}) + R_{ij}B\left(\mathbf{v}_i,\mathbf{v}_j\right) + \mathbf{F}. \tag{19}$$

This is exactly the mean field equation produced by the QG methodology.

- *Evolution of the QG covariance matrix*

To approximate the QG covariance matrix, we will use the (exact) equation for the fixed basis (4). This can also be written as

$$\frac{dR}{dt} = L_v R + RL_v^* + Q_F + Q_\sigma, \tag{20}$$

where L_v is the linearized dynamics operator given by (6), Q_σ is the positive energy transfer due to external noise given by (7), and Q_F is the flux of energy connected (see Eq. (8)) to the unknown third-order statistics defined over the space $\mathbb{R}^N$ spanned by $\mathbf{v}_i$, $i = 1,\ldots,N$.

Note that the equation for the covariance can also be seen as a generalized Kármán–Howarth relation [23], which is used for the connection of the third-order statistics and the energy content of a system in the steady state. The straightforward computation of the third-order statistics involves a closure problem which we will not handle directly. In contrast to the QG method, where this quantity is set to zero, in this blended QG–DO approach this quantity will be approximated through a reduced-order DO approach that will run in parallel to the above two equations for the mean and covariance.

Specifically, we will approximate the energy flux Q_F using the reduced-order DO basis. Then, the DO reduced-order energy flux will be given by

$$\begin{aligned} Q_F \simeq Q_{F,s} &= \left\langle B\left(\mathbf{u}',\mathbf{u}'\right)\cdot\mathbf{v}_i Z_j\right\rangle \\ &= \langle Y_m Y_n Y_l\rangle\,(B(\mathbf{e}_m,\mathbf{e}_n)\cdot\mathbf{v}_i)\left(\mathbf{v}_j\cdot\mathbf{e}_l\right) \\ &\quad + \langle Y_m Y_n Y_l\rangle\left(B(\mathbf{e}_m,\mathbf{e}_n)\cdot\mathbf{v}_j\right)(\mathbf{v}_i\cdot\mathbf{e}_l). \end{aligned} \tag{21}$$

The above quantity expresses the energy fluxes to any element of the high-dimensional fixed subspace from the DO reduced-order subspace only. This equation can be used to study energy transfer properties from the stochastic subspace to the orthogonal complement and vice versa. Using this approach, we have not performed reduction on the dynamics of the system but only on the way the energy fluxes are computed.

We emphasize that, for systems with persistent instabilities in the linearized dynamics, and with sufficiently low-dimensional DO subspace, the nonlinear fluxes Q_F may not be adequately modeled by $Q_{F,s}$, since some unstable modes may not be contained in the stochastic subspace. In this case, we may have large approximation error, and another approach should be followed in which the QG closure scheme is substituted by a modified QG closure (see [22,24]). However, in the present work, we assume that the linearized dynamics are stable, and that the system energy is mainly due to external noise and not due to internal instabilities.

- *Evolution of the DO stochastic subspace and stochasticity*

The evolution of the DO basis should not be influenced by the fact that we consider a higher (than s) dimensional space. This is because, if we include on the right-hand side of the DO basis equations the extra dimensions resolved using the QG model, then the stochastic subspace will not move towards these directions (in general, the subspace tends to capture directions associated with higher energy). Thus we keep the DO basis equation as it is:

$$\begin{aligned} \frac{\partial\mathbf{e}_l}{\partial t} &= [L+D]\,\mathbf{e}_l + B(\bar{\mathbf{u}},\mathbf{e}_l) + B(\mathbf{e}_l,\bar{\mathbf{u}}) \\ &\quad + \sum_{n_1,n_2,n_3=1}^{s} B\left(\mathbf{e}_{n_2},\mathbf{e}_{n_3}\right)\left\langle Y_{n_1}Y_{n_2}Y_{n_3}\right\rangle C^{-1}_{ln_1} \\ &\quad - \mathbf{e}_m\Bigg([L+D]\,\mathbf{e}_l + B(\bar{\mathbf{u}},\mathbf{e}_l) + B(\mathbf{e}_l,\bar{\mathbf{u}}) \\ &\quad + \sum_{n_1,n_2,n_3=1}^{s} B\left(\mathbf{e}_{n_2},\mathbf{e}_{n_3}\right)\left\langle Y_{n_1}Y_{n_2}Y_{n_3}\right\rangle C^{-1}_{ln_1}\Bigg)\cdot\mathbf{e}_m. \end{aligned} \tag{22}$$

In addition, the evolution of uncertainty within the stochastic subspace is performed using equations that come directly from the Galerkin projection to the time-evolving subspace. Note that, although we do not have terms representing the effect of the orthogonal complement dynamics on the stochastic subspace, we have an implicit influence through the mean field,

$$\begin{aligned} \frac{dY_l}{dt} &= Y_m\left([L+D]\,\mathbf{e}_m + B(\bar{\mathbf{u}},\mathbf{e}_m) + B(\mathbf{e}_m,\bar{\mathbf{u}})\right)\cdot\mathbf{e}_l \\ &\quad + \left(Y_m Y_n - C_{mn}\right)B(\mathbf{e}_m,\mathbf{e}_n)\cdot\mathbf{e}_l + \dot{W}_p\sigma_p\cdot\mathbf{e}_l. \end{aligned} \tag{23}$$

To summarize, we propose the closed set of Eqs. (19)–(23) as a new blended QG–DO UQ method for systems with stable mean state. Although the method is described for systems having the form (1), the QG–DO approach can be applied to more generic cases such as higher-order nonlinearities, multiplicative noise, etc. This blended approach overcomes the disadvantages of each of the methods that it is based on. In particular, we have a UQ

methodology that evolves the second-order characteristics in a fixed basis, while it computes the non-Gaussian characteristics only for high-energy time-dependent modes, described by the DO field equations. This non-Gaussian reduced-order information is used for the computation of the energy fluxes and the evolution of the second-order structure in the high-dimensional fixed basis subspace. Finally, it is worth remarking here that, for blended QG–DO algorithms with $s = 1$ and a single mode in DO, with (17), essentially the QG closure is recovered, with a Monte Carlo algorithm in the one-dimensional subspace.

6. Application of the blended QG–DO method to the triad system

We consider the triad system in various configurations as previously, including non-normal linearized dynamics and strong energy cascade regimes. To assess the performance of the developed UQ algorithm, we also consider time-dependent excitations that drive the system between regimes of equipartition of energy (with zero nonlinear energy transfers and Gaussian statistics) and regimes of strong energy cascade (with strongly non-Gaussian characteristics).

More specifically, we will be using time-dependent noise intensity and forcing. In particular, we will consider the following more generic (than (16a)–(16c)) time-dependent triad system:

$$\begin{aligned} du_1 &= (-\gamma_1 u_1 + \lambda_{12} u_2 + \lambda_{13} u_3 + \beta_1 u_3 u_2 + g)\, dt \\ &\quad + \left(\sigma_1 + f^2 (\sigma_{T1} - \sigma_1)\right) dW_1 \\ du_2 &= (-\gamma_2 u_2 - \lambda_{12} u_1 + \lambda_{23} u_3 + \beta_2 u_1 u_3 + g)\, dt \\ &\quad + \left(\sigma_2 + f^2 (\sigma_{T2} - \sigma_2)\right) dW_2 \\ du_3 &= (-\gamma_3 u_3 - \lambda_{13} u_1 - \lambda_{23} u_2 + \beta_3 u_2 u_1 + g)\, dt \\ &\quad + \left(\sigma_3 + f^2 (\sigma_{T3} - \sigma_3)\right) dW_3, \end{aligned}$$

where f^2 and g are time-dependent functions and $\sigma_{Ti} > \sigma_i$. Below, we give a summary of all the cases that we present.

- *Strongly nonlinear regime with Gaussian steady state:* This case has fixed-in-time parameters ($f = 0$) and zero mean forcing ($g = 0$). The parameters are chosen so that

$$\frac{\sigma_1^2}{2\gamma_1} = \frac{\sigma_2^2}{2\gamma_2} = \frac{\sigma_3^2}{2\gamma_3} = E. \tag{24}$$

  This particular constraint results in a Gaussian steady state with equipartition of energy.
- *Strongly nonlinear regime with an energy cascade:* This case also has fixed-in-time parameters ($f = 0$) and zero mean forcing ($g = 0$). The parameters are chosen so that

$$\gamma_1 \ll \gamma_2, \gamma_3 \quad \text{and} \quad \sigma_1 \gg \sigma_2, \sigma_3. \tag{25}$$

  This particular constraint results in strong energy transfer from the first degree of freedom to the second and third degrees of freedom (Fig. 4). This strong energy transfer is also manifested by the strongly non-Gaussian properties of the steady-state probability measure.
- *Time dependent parameters I: Periodic and step-function dependence:* For this case, we use time-dependent parameters. We consider two cases: $f(t) = g(t) = \sin\left(\frac{\pi}{4}t\right)$, and $f(t) = H(t - T)$, where H is the Heaviside function. The parameters $\sigma_1, \sigma_2, \sigma_3$ are chosen to satisfy condition (25), and the parameters $\sigma_{T1}, \sigma_{T2}, \sigma_{T3}$ satisfy condition (24), so that the system oscillates between two regimes of completely different behavior.
- *Time-dependent parameters II: Stochastic time dependence:* In this case, we also use time-dependent parameters, but this time $f(t)$ and $g(t)$ are Ornstein–Uhlenbeck processes described by the equation

$$df = -\frac{1}{T} f + a\sqrt{\frac{2}{T}} dW.$$

  The correlation time is chosen as $T = 2$, and we also choose $a = 0.5$; this choice produces random series having maxima of $O(1)$. The noisy intensity is set as in the previous case, so that we have random transitions between the energy cascade regime and the equipartition regime.

Strongly nonlinear regime with Gaussian steady state

In this case of parameters, the system reaches a statistical equilibrium in which all directions of phase space have equal amount of energy. As we saw in Section 4, where the limitations of order reduction were illustrated, single-mode reduction performs badly for this set of parameters. In Fig. 5 (upper-left panel), we also present the results for the two-mode DO reduction, and the same conclusions can be made for the UQ performance during convergence to the statistical steady state. We observe (upper-right panel) that in both cases ($s = 1, 2$) the DO algorithm captures the variance inside the subspace correctly. However, the amount of variance that is omitted is sufficient to create discrepancies in the mean values.

This is not the case for the QG and blended QG–DO algorithms (second row), where the estimated and exact mean values compare favorably, as can be seen from the second row of Fig. 5. To get a more accurate picture of the performance of the algorithms, we use the information distance between the approximation $\mathbf{u}$ and the Monte Carlo solution υ by applying (14) on the whole space [13,10]. As can be seen in the lower-left plot, both algorithms are performing equally well. The very good performance of the QG closure was expected for this case if we take into account the Gaussian character of the invariant probability measure which results in the absence of any nonlinear energy transfer properties between modes (recall that the nonlinear fluxes Q_F depend on the third-order moments—Eq. (8)). In the next numerical experiment, we will see that the presence of the latter feature may create important errors in the QG algorithm.

Strongly nonlinear regime with an energy cascade

In this configuration, the parameters are chosen so that strong energy transfer occurs from one high-energy mode to the other two low-energy modes. The performance of the various UQ approaches considered in this paper are shown in Fig. 6. In the first row, we can clearly see the limitations of the order-reduction approach. The absence of even one mode does not allow for the approximation scheme to reach a statistical equilibrium. Moreover, the DO modes continuously oscillate, creating artificial fluctuations in the amount of variance in the subspace.

On the other hand, we see that the QG and QG–DO methods overcome these limitations. In particular, the QG–DO method with a two-dimensional subspace gives the best performance (see the information distance panel in Fig. 6), since it captures the energy transfers from the high-energy mode to the other two modes. In contrast, the QG method, by construction, cannot capture any nonlinear energy transfers, and the information distance grows monotonically as a result of this continuous error. With our remark at the end of Section 5.2, it is not surprising that the QG–DO method with $s = 1$ behaves similarly to the QG method.

In the bottom-right panel of Fig. 6 we also present the pdf inside the DO subspace (for $s = 2$) after the system has reached a statistical equilibrium. The pdf had been visualized using a histogram on the samples of the stochastic coefficients (Y_1, Y_2). This is compared with the corresponding histogram of the projection of the Monte Carlo realizations to the QG–DO subspace with $s = 2$, and it is clear that the QG–DO method captures these non-Gaussian statistics very well.

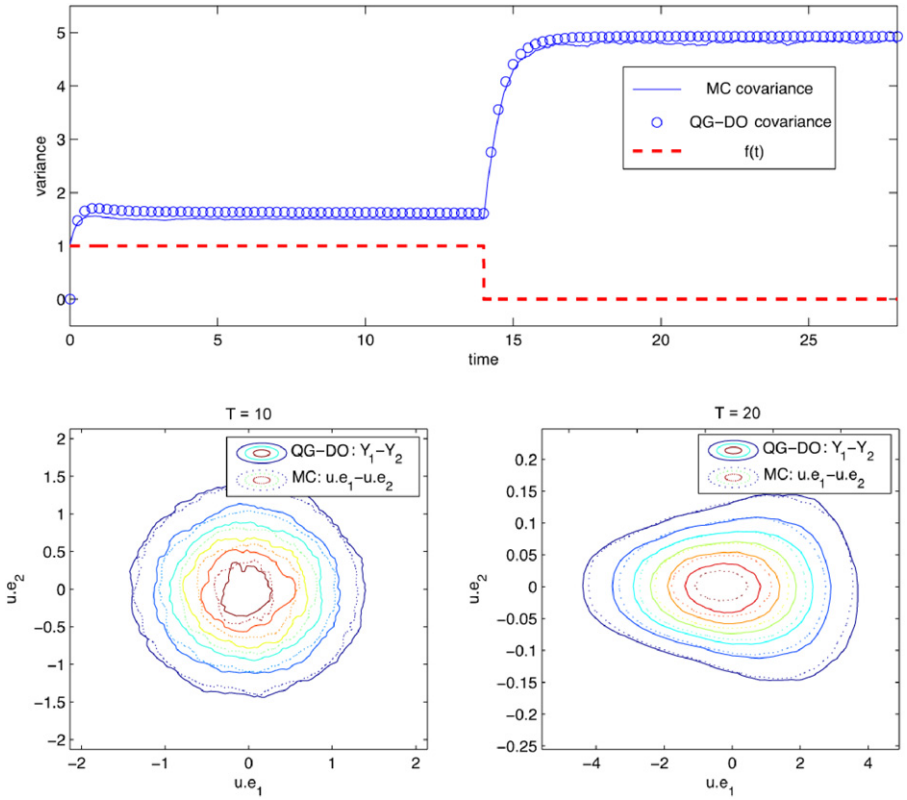

Fig. 7. Trace of covariance and pdf in V_S resolved with the QG–DO method ($s = 2$) for the case of step-function time dependence $f(t)$ on the parameters.

Time-dependent parameters I: step-function and periodic dependence

Here we validate our UQ algorithms for a time-dependent set of system parameters. In particular, the system parameters change suddenly from a set that corresponds to a Gaussian steady state to one that corresponds to a strongly non-Gaussian steady state with an energy cascade. The results are shown in Fig. 7 in terms of the covariance trace and the response pdf inside the stochastic subspace. In both regimes, the QG–DO method with a two-dimensional subspace compares very well with the direct Monte Carlo simulation. The next numerical experiment involves the same setup as previously, but with periodic variation of the system parameters as well as with deterministic periodic forcing. The results are shown in Fig. 8. Direct DO reduction creates important error in both the first-order and second-order statistics. Additionally, from the form of the captured variance (upper-right panel), it is clear that the modes follow an aperiodic trajectory since the captured covariance time series is non-periodic.

On the other hand, the QG method has surprisingly good performance, given that it does not capture any nonlinear energy transfers. This can clearly be seen from the information distance panel, where the QG and QG–DO ($s = 1$) discrepancies are presented during the temporal regimes where the system parameters correspond to strong nonlinear energy transfers. For a two-dimensional subspace, the blended QG–DO method reduces this error significantly, since it captures a large part of the non-Gaussian structure and thus it models an important portion of the nonlinear energy fluxes.

Time-dependent parameters II: random dependence

In the final numerical experiment that we consider, the system parameters fluctuate stochastically (see the beginning of the section for a detailed description) between a set that corresponds to strong energy transfers and one where we have Gaussian statistics (zero energy transfers). The results are presented in Fig. 9. We observe that both the first-order and second-order properties of the system present strong fluctuations. In contrast to the standard DO method, the QG and the QG–DO methods are able to track very well the variations of the system statistics. Moreover, in a similar manner to the previous numerical experiment, the QG–DO method with the two-dimensional subspace outperforms the QG and QG–DO $s = 1$ methods in the regimes where strong energy transfers are present (i.e. regimes where $f(t) \simeq 0$).

The above numerical experiments illustrate clearly the need to consider, even through a very simplified and inexpensive approach like the QG method, the maximum number of relevant modes so that we capture essentially irreducible features such as non-normal dynamics or important variance in modes that essentially behave linearly (i.e. they do not interact with other modes). Nonlinear interactions such as energy transfers between modes require knowledge of the non-Gaussian structure, and, as we saw in this case, the blending of the QG closure with a non-Gaussian reduced-order DO algorithm provides an inexpensive approach for UQ in such systems.

Application of the QG–DO method to large-dimensional systems

The direct use of the QG closure in the blended QG–DO algorithm is impractical for $\mathbf{u} \in \mathbb{R}^N$ with $N \gtrapprox 1000$. In this important practical situation, one can choose the $\{\mathbf{v}_i\}_{i=1}^M$ to span a fixed M-dimensional subspace with M sufficiently large and repeat the derivation of the QG–DO algorithm. This subspace can be chosen, for example, to capture both intermittency and low-frequency variability through the NLSA algorithm [7].

7. Conclusions and future directions

Reduced-order modeling has been proven successful for describing a variety of systems that have low-dimensional attractors.

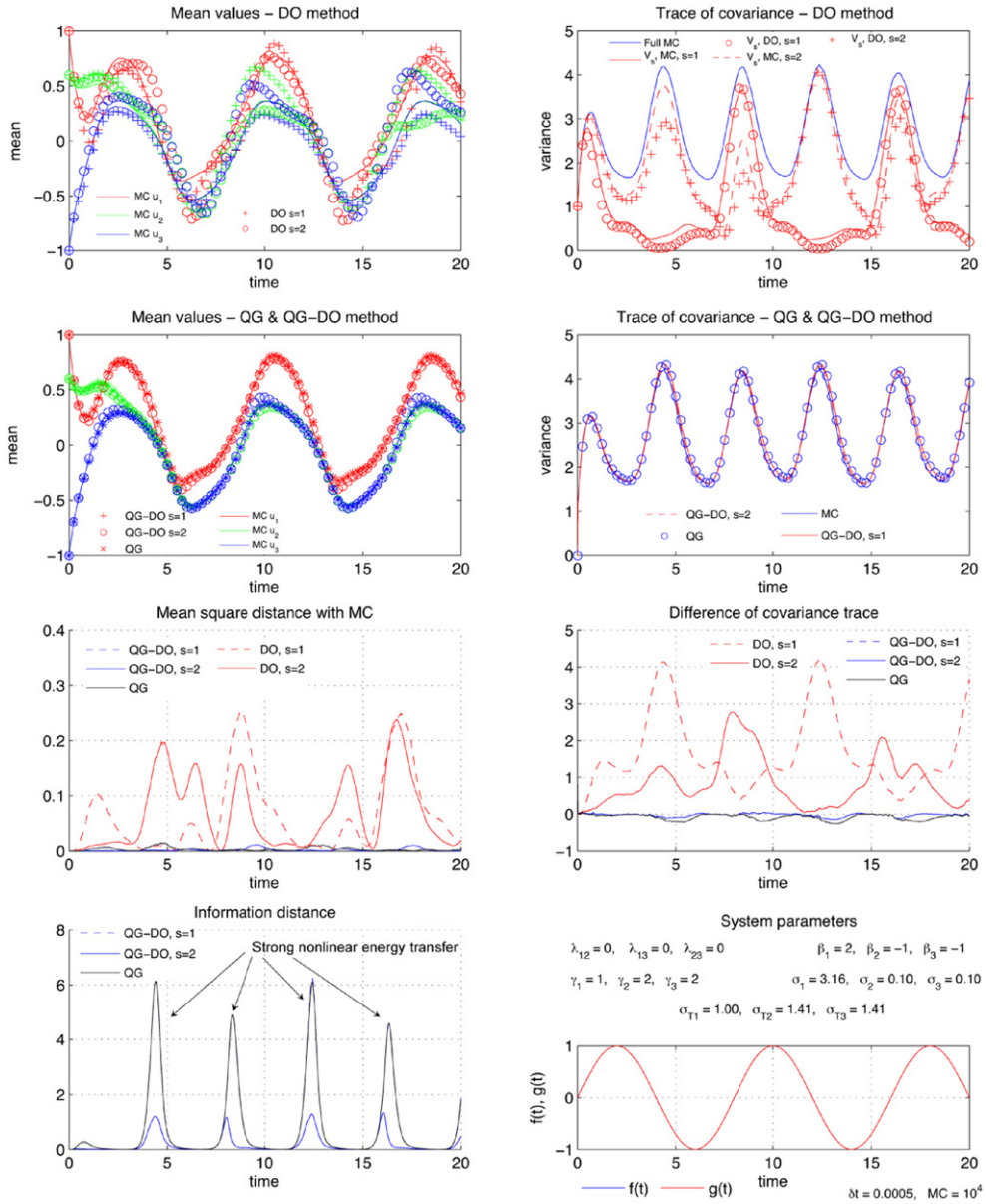

Fig. 8. Comparison of the considered UQ algorithms for the triad system for periodic dependence of system parameters. The time-series results are presented in terms of the first and second moments, and they are compared with direct Monte Carlo simulations.

Here, we have analyzed and illustrated generic limitations of order reduction in dynamical systems with essentially irreducible features. Such features as non-normal dynamics, variance over a wide range of modes, and energy transfers due to nonlinear terms are typical in realistic applications involving turbulent fluid flows and advection of passive tracers. The quantification of the UQ performance was done using an empirical information framework as well as through more standard measures.

Subsequently, we developed a blended method using two existing approaches. The first ingredient was the classic quasilinear Gaussian closure, which is an inexpensive way to model a wide range of modes, although the underlying Gaussian assumption ignores important energy transfers (connected with third-order moments) that may be present in systems with strong nonlinearities such as those that we consider. This important drawback of the QG method was overcome by blending this inexpensive approach with the DO framework that models the full non-Gaussian statistical features, but only for a low-dimensional stochastic subspace. The blending of the methods resulted in a new approach that overcomes the limitations of its two ingredients and performs well and inexpensively in modeling strong energy transfers associated with non-Gaussian statistics. Beyond the very good performance in capturing second-order statistics over the full phase space, the blended method was also able to provide accurate high-order statistical information within the stochastic subspace.

Our analysis was restricted to systems in which the finite size of the stochastic attractor is due to the external stochastic excitation only, i.e. systems with stable mean state. This limitation is due to the choice of the QG method (as one of the ingredients of the blended approach) which cannot handle systems with persistent internal instabilities [22]. Therefore, a different approach should be followed, based on the blending of a modified quasilinear Gaussian closure and reduced-order subspace techniques as DO. Results along this direction will be reported by the authors in the near future [24].

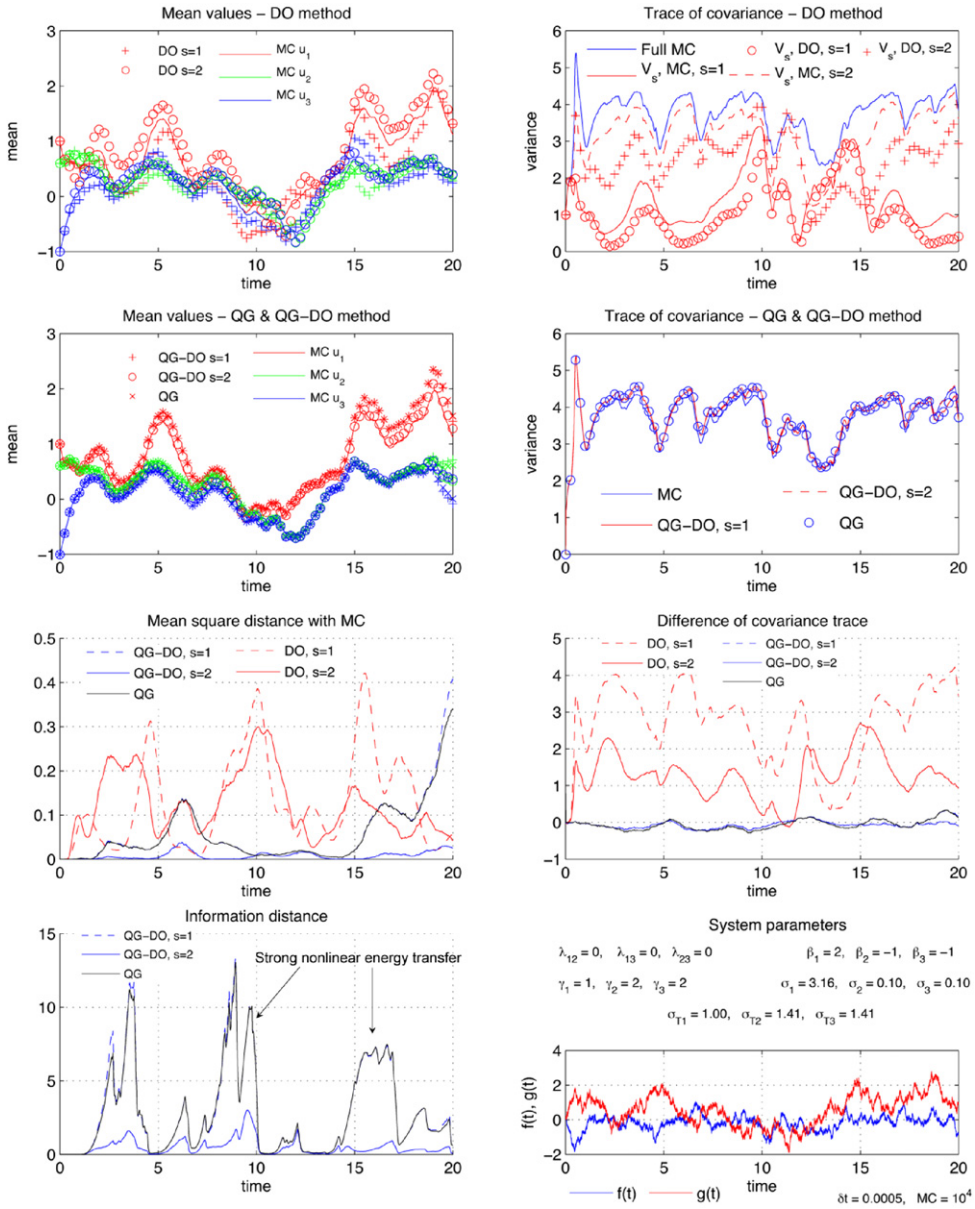

Fig. 9. Comparison of the considered UQ algorithms for the triad system for random dependence of system parameters. The time-series results are presented in terms of the first and second moments, and they are compared with direct Monte Carlo simulations.

Acknowledgments

The research of A. Majda is partially supported by NFS grant DMS-0456713, NSF CMG grant DMS-1025468, and ONR grants ONR-DRI N00014-10-1-0554 and N00014-11-1-0306. T. Sapsis is supported as a postdoctoral fellow on the first and third grants.

References

[1] L. Sirovich, Turbulence and the dynamics of coherent structures, parts I, II and III, Quart. Appl. Math. XLV (1987) 561–590.
[2] P. Holmes, J. Lumley, G. Berkooz, Turbulence, Coherent Structures, Dynamical Systems and Symmetry, Cambridge University Press, 1996.
[3] S. Lall, J.E. Marsden, S. Glavaski, A subspace approach to balanced truncation for model reduction of nonlinear control systems, Internat. J. Robust Nonlinear Control 12 (2002) 519.
[4] Z. Ma, C.W. Rowley, G. Tadmor, Snapshot-based balanced truncation for linear time-periodic systems, IEEE Trans. Automat. Control 55 (2010) 469.
[5] T.P. Sapsis, P.F.J. Lermusiaux, Dynamically orthogonal field equations for continuous stochastic dynamical systems, Physica D 238 (2009) 2347–2360.
[6] T.P. Sapsis, Attractor local dimensionality, nonlinear energy transfers, and finite-time instabilities in stochastic dynamical systems with applications to 2D fluid flows, Proc. R. Soc. A 469 (2013) 2153.
[7] D. Giannakis, A.J. Majda, Nonlinear Laplacian spectral analysis for time series with intermittency and low-frequency variability, Proc. Natl. Acad. Sci. 109 (2012) 2222.
[8] G. Tadmor, O. Lehmann, B.R. Noack, M. Morzynski, Mean field representation of the natural and actuated cylinder wake flow, Phys. Fluids 22 (2010) 034102.
[9] G. Tadmor, O. Lehmann, B.R. Noack, L. Cordier, J. Delville, J.P. Bonnet, M. Morzynski, Reduced order models for closed-loop wake control, Phil. Trans. R. Soc. A 369 (2011) 1513–1524.
[10] A.J. Majda, B. Gershgorin, Quantifying uncertainty in climate change science through empirical information theory, Proc. Natl. Acad. Sci. 107 (2010) 14958.
[11] A.J. Majda, Challenges in climate science and contemporary applied mathematics, Comm. Pure Appl. Math. 65 (2012) 920.
[12] A.J. Majda, X. Wang, Nonlinear Dynamics and Statistical Theories for Basic Geophysical Flows, Cambridge University Press, 2006.
[13] A.J. Majda, M. Branicki, Lessons in uncertainty quantification for turbulent dynamical systems, Discrete Contin. Dyn. Syst. 32 (2012) 3133–3221.
[14] T.P. Sapsis, H.A. Dijkstra, Interaction of noise and nonlinear dynamics in the double-gyre wind-driven ocean circulation, J. Phys. Oceanogr. 43 (2013) 366.
[15] M.P. Ueckermann, P.F.J. Lermusiaux, T.P. Sapsis, Numerical schemes for dynamically orthogonal equations of stochastic fluid and ocean flows, J. Comput. Phys. 233 (2013) 272–294.
[16] T.P. Sapsis, P.F.J. Lermusiaux, Dynamical criteria for the evolution of the stochastic dimensionality in flows with uncertainty, Physica D 241 (2012) 60.
[17] E. Lorenz, Maximum simplification of the dynamic equations, Tellus 12 (1960) 243.

[18] A.J. Majda, I. Timofeyev, E. Vanden-Eijnden, Models for stochastic climate prediction, Proc. Natl. Acad. Sci. 96 (1999) 14687.
[19] A.J. Majda, I. Timofeyev, E. Vanden-Eijnden, A mathematical framework for stochastic climate models, Comm. Pure Appl. Math. 54 (2001) 891.
[20] A.J. Majda, I. Timofeyev, E. Vanden-Eijnden, A priori tests of a stochastic mode reduction strategy, Physica D 170 (2002) 206.
[21] G.L. Eyink, F.J. Alexander, Predictive turbulence modeling by variational closure, J. Stat. Phys. 91 (1998) 221.
[22] T.P. Sapsis, A.J. Majda, Blended reduced subspace algorithms for uncertainty quantification of quadratic systems with a stable mean state, Physica D (2013) in press.
[23] U. Frisch, Turbulence, The Legacy of A. N. Kolmogorov, Cambridge University Press, 1996.
[24] T.P. Sapsis, A.J. Majda, Blending modified Gaussian closure and non-Gaussian reduced subspace methods for turbulent dynamical systems, J. Nonlinear Sci. (2013) submitted for publication.